

Effect of Impurities and Effective Masses on Spin-Dependent Electrical Transport in Ferromagnet-Normal Metal-Ferromagnet Hybrid Junctions

Zhen-Gang Zhu, Gang Su*, Biao Jin and Qing-Rong Zheng
Department of Physics, The Graduate School of the Chinese Academy of Sciences, P.O. Box 3908, Beijing 100039, China

Abstract

The effect of nonmagnetic impurities and the effective masses on the spin-dependent transport in a ferromagnet-normal metal-ferromagnet junction is investigated on the basis of a two-band model. Our results show that impurities and the effective masses of electrons in two ferromagnetic electrodes have remarkable effects on the behaviors of the conductance, namely, both affect the oscillating amplitudes, periods, as well as the positions of the resonant peaks of the conductance considerably. The impurity tends to suppress the amplitudes of the conductance, and makes the spin-valve effect less obvious, but under certain conditions the phenomenon of the so-called impurity-induced resonant tunneling is clearly observed. The impurity and the effective mass both can lead to nonmonotonous oscillation of the junction magnetoresistance (*JMR*) with the incident energy and the thickness of the normal metal. It is also observed that a smaller difference of the effective masses of electrons in two ferromagnetic electrodes would give rise to a larger amplitude of the *JMR*.

PACS numbers: 75.70. Cn, 73.40.Jn, 73.40.Gk

I. INTRODUCTION

It is getting realized that the successful control of spin-polarized electrical currents would give rise to essential impact in information technology, thereby resulting in that the spin-dependent tunneling in hybrid systems of ferromagnetic and normal metals (insulators) has attracted much attention during the past years (see, e.g. Refs. [1–4] for review). A nascent field dubbed as *spintronics*, is therefore emerging. Among others, a large number of studies on the electrical transport properties in metallic magnetic multilayers show the existence of the effect of a so-called giant magnetoresistance (GMR) [5], which is now believed to be caused by spin-dependent scattering in the systems. Since its potential applications, the GMR effect has been actively studied both theoretically and experimentally in recent years (see, e.g. Refs. [2,6]).

Apart from the GMR found in metallic magnetic multilayers, the spin-valve effect is observed in ferromagnetic (FM) tunneling junctions. Following the discovery of spin-polarized tunneling of conduction electrons in ferromagnets by Tedrow and Meservey [7], Jullière was the first to observe the effect that the tunneling resistance in an F-I-F junction consisting of two FM electrodes separated by an insulating (I) barrier depends strongly on the relative orientations of magnetizations, namely the resistance is low when magnetizations in FM electrodes are parallel, and the resistance is high when magnetizations in FM electrodes are antiparallel, and a two-current model was proposed to interpret the observed large junction magnetoresistance in Fe-Ge-Co junctions at 4.2 K by assuming the spin conservation so that the tunneling of spin up and spin down electrons undergoes two independent processes [8]. The tunneling magnetoresistance has also been observed by Maekawa and Gäfvert [9]. Treating the F-I-F junction as a single quantum-mechanical system, Slonczewski adopted a free-electron model to describe the tunneling of spin-polarized conduction electrons, and recovered the spin-valve effect [10]. The extension of Slonczewski's model to a realistic band structure based on a tight-binding model was established [11]. Recently, on the basis of scattering matrix theory the spin-dependent electrical and thermal transport in F-I-F junctions was developed at finite bias voltage and at finite temperatures [12]. It is found that not only the electrical conductance but also the thermal conductance reveals the spin-valve effect at low temperatures. There are also some theories devoted to F-I-F tunneling junctions (see Ref. [4] for a review). Moreover, the spin-valve effect can also appear in ferromagnet-normal metal-ferromagnet (F-N-F) junctions which may have different transport properties from the F-I-F junctions. Johnson was the first to predict the phenomenon of spin accumulation in F-N-F junctions, which was soon confirmed in a three-terminal device, and a transistor effect was observed in such a device [13]. Valet and Fert studied the F-N-F structure and applied the Boltzmann equation to the current perpendicular to the plane structure by assuming that the thickness of nonmagnetic metallic layer is much shorter than the spin-diffusion length. The theory can reduce to Johnson's theory as the thickness of nonmagnetic metal is much longer than the spin-diffusion length [14]. By taking into account different magnetizations of ferromagnetic reservoirs and spin diffusion in the normal metal, Hernando et al studied the equation for the diffusive spin transport in the F-N-F structure and showed that the difference between the conductance of the parallel and antiparallel configuration can be either positive or negative as a function of the applied magnetic field [15]. Zheng et al have investigated a double tunnel junction model describing the F-I-N-I-F structure

by means of quantum mechanical approach, and the oscillation of the tunneling conductance and the TMR on the spacer's thickness is found [16]. A finite-element method [17] and nonequilibrium Green function method [18] has also been applied to the mesoscopic junction systems.

Within the theories above mentioned, the effect of impurities was not much investigated. Although it is argued that the impurities and defects may lead to the resonant tunneling in F-I-F junctions [19], the study on the effect of impurities on the spin-dependent transport in F-N-F junctions is still sparse. Another important factor, which is usually ignored in theories, is the effect of the effective masses of electrons in FM and normal layers. As in realistic hybrid junctions the electrodes are made by different ferromagnets, such as half-metals [19] and magnetic semiconductors [20–22], the effective mass would have significant effect on the transport properties. In this paper, by treating the F-N-F junction as a quantum-mechanical system we shall investigate the effect of nonmagnetic impurities as well as the effective masses of electrons in FM and normal layers on the spin-dependent electrical transport properties in spin-valve systems. It is found that the impurity and the effective mass can both lead to nonmonotonous oscillation of *JMR* with the incident energy and the thickness of the normal metal. The effective mass can enlarge the *JMR* effect when the difference between the two FM layers is small. On the other hand, if the difference is large, the *JMR* effect becomes smaller and the inverse *JMR* effect would appear.

The rest of this paper is outlined as follows. In Sec. II the model which we shall adopt in the subsequent sections will be described and some relevant formalism will be derived. Sec. III will present the effect of nonmagnetic impurities on the junction magnetoresistance in F-N-F junctions, and the effect of effective masses of electrons in FM electrodes will be given in Sec. IV. Finally, a summary will be presented.

II. MODEL AND FORMALISM

Consider an F-N-F junction consisting of two ferromagnetic layers separated by a normal metal layer with thickness d . In a nearly-free-electron approximation of the spin-polarized conduction electrons, the longitudinal part of the effective one-electron Hamiltonian can be written as

$$H = -\frac{\hbar^2}{2m_j^*} \frac{d^2}{dx^2} + U(x) + [\gamma_1 \delta(x) + \gamma_2 \delta(x - d)] - \mathbf{h}(j) \cdot \sigma \quad (1)$$

where m_j^* ($j = 1, 2, 3$) is the effective mass of an electron in three regions (Region 1: left FM electrode; Region 2: normal metal; Region 3: right FM electrode), respectively. The potential $U(x)$ is composed of three parts: a small bias voltage V , two contact potentials V_1 and V_2 defined as $U(x) = V_1$ for $x \leq 0$, $U(x) = V_2$ for $x \geq d$ and zero otherwise. The contact potentials between the ferromagnetic layers and the normal metallic layer could be effectively considered to be caused either by roughness of interfaces or by two equivalent, thin insulating layers. $\mathbf{h}(j)$ represents the molecular field in FM electrodes, and σ is the conventional Pauli matrices. By assumption, $\mathbf{h} = 0$ inside the nonmagnetic normal metal. In FM electrodes $\mathbf{h} = \mathbf{h}_L$ or \mathbf{h}_R is constant with relative orientation labeled by angle θ . The potentials induced by impurities or defects on the interfaces between the ferromagnetic and

nonmagnetic metal layers have been discussed in Ref. [23]. Generally speaking, the delta-potentials of impurities or defects on interfaces depend on three-dimensional coordinates. To simplify the problem and to get useful analytical results, the potentials are supposed to have forms of δ potentials as shown in Eq. (1) where γ_1 and γ_2 are corresponding coefficients. We expect that such an approximation would not cause significant qualitative changes on the interested transport properties, as the motion of electrons along the transverse direction are not emphasized in the present approach. The schematic layout of the F-N-F junction is depicted in Fig. 1. Inside the ferromagnets, a two-band model will be used to describe the motion of spin-polarized electrons. As spin up and spin down bands are split by exchange interactions, the electrons with spin up and down have different energies in FM electrodes, and the one-electron energy is $E_{1x} = \hbar^2 k_{1\sigma}^2 / 2m_1^* - \sigma h_L + V_1$ for the left FM electrode, and $E_{3x} = \hbar^2 k_{3\sigma}^2 / 2m_3^* - \sigma h_R + V_2$ for the right FM electrode with $\sigma = \pm 1$ corresponding to $\sigma = \uparrow, \downarrow$ respectively. Inside the nonmagnetic normal metal layer, the one-electron energy is $E_{2x} = \hbar^2 k^2 / 2m_2^*$.

Consider an incident plane wave of spin-up electrons with unit flux in Region 1. The solution of the Schrödinger equation with eigenvalue E_{1x} in the region of the left FM electrode can be written as

$$\psi_{1\uparrow} = k_{1\uparrow}^{-1/2} e^{ik_{1\uparrow}x} + R_{\uparrow} e^{-ik_{1\uparrow}x}, \quad \psi_{1\downarrow} = R_{\downarrow} e^{-ik_{1\downarrow}x}. \quad (2)$$

In the normal metal region, the eigenfunctions of H with eigenvalue E_{2x} are written as

$$\psi_{2\sigma} = A_{\sigma} e^{ikx} + B_{\sigma} e^{-ikx}, \quad \sigma = \uparrow, \downarrow. \quad (3)$$

In the region of the right FM electrode, the eigenfunctions of H with eigenvalue E_{3x} have the form

$$\psi_{3\sigma} = C_{\sigma} e^{ik_{3\sigma}(x-d)}, \quad \sigma = \uparrow, \downarrow. \quad (4)$$

The coefficients $R_{\uparrow}, R_{\downarrow}, A_{\sigma}, B_{\sigma}, C_{\sigma} (\sigma = \pm 1)$ are to be determined by properly matching $\psi_{j\sigma}$ and $d\psi_{j\sigma}/dx$ at the interfaces $x = 0$ and $x = d$ (the boundary conditions). Owing to the spin conservation the spin directions are fixed as the electrons move from Region 1 to Region 2. The existence of δ -like impurity potential at the interfaces makes the derivatives of wave functions no longer continuous. For the simplicity we shall set $m_1^* = m_2^* = m_3^* = m$ first, and then consider the effect of different effective masses in Sec. IV. At the interface $x = 0$, the boundary condition is

$$\psi_1(0) = \psi_2(0), \quad \frac{d\psi_2(0)}{dx} - \frac{d\psi_1(0)}{dx} = \mu_1 \psi_2(0), \quad (5)$$

where $\mu_1 = \frac{2m_2^* \gamma_1}{\hbar^2}$. At the interface $x = d$, the boundary condition is

$$\psi_2(d) = \Re \psi_3(d), \quad \frac{d\psi_2(d)}{dx} = \Re \left[\frac{d\psi_3(d)}{dx} - \mu_2 \psi_3(d) \right], \quad (6)$$

where the rotation matrix $\Re = \begin{pmatrix} \cos \frac{\theta}{2} & \sin \frac{\theta}{2} \\ -\sin \frac{\theta}{2} & \cos \frac{\theta}{2} \end{pmatrix}$ and $\mu_2 = \frac{2m_3^* \gamma_2}{\hbar^2}$. In accordance with Eqs. (2)-(6), all unknown coefficients introduced above can be obtained. The results are collected

in Appendix, where the quantities $q_1(\equiv \frac{m_2^*}{m_1^*}) = q_2(\equiv \frac{m_3^*}{m_2^*}) = 1$ should be taken due to the assumption of the same effective masses here. (The case $q_1 \neq q_2$ will be discussed later.) In comparison to the results in F-I-F junctions as discussed by Slonczewski [10], our equations (3), (5) and (6) for F-N-F junctions with impurities are quite different. It is these differences that enable the transport properties in two kind of junctions to show different behaviors.

The transmissivity $T_{p\sigma} = \text{Im} \sum_{\sigma} \psi_{\sigma}^*(d\psi_{\sigma}/dx)$ can be derived analytically

$$T_{p\uparrow} = \frac{R_{\downarrow}^* R_{\downarrow}}{4(a_3 - a_4)^2} \left[\frac{k_{3\uparrow}(c_{31}^2 + c_{32}^2)}{\sin^2 \frac{\theta}{2}} + \frac{k_{3\downarrow}(c_{61}^2 + c_{62}^2)}{\cos^2 \frac{\theta}{2}} \right], \quad (7)$$

where R_{\downarrow} , a_3 , a_4 , c_{31} , c_{32} , c_{61} , c_{62} are given in the Appendix. $T_{p\uparrow}$ is valid for spin-up incident electrons and $T_{p\downarrow}$ is valid for spin-down electrons by the same expression as Eq.(7) with $k_{1\uparrow}$ and $k_{1\downarrow}$, $k_{3\uparrow}$ and $k_{3\downarrow}$ interchanged. Thus the total transmissivity in the two-band case, $T_p(\theta) = T_{p\uparrow}(\theta) + T_{p\downarrow}(\theta)$, may be obtained.

At zero temperature, it can be reasonably assumed that the electrons with E_x near Fermi energy E_F carry most of the current. With this assumption and by summing the charge transmission over E_x and \mathbf{k}_{\parallel} for the occupied states in the usual manner [24], one can find the conventional expression of surface conductance at a small bias voltage

$$G(\theta) = \frac{I_e}{V} = \frac{m_1^* e^2}{2\pi^2 \hbar^3} E_F T_p(\theta), \quad (8)$$

where $m_1^* = m_2^* = m_3^* = m$. The junction magnetoresistance (JMR) is defined as usual

$$JMR(\theta) = \frac{G(\theta = 0) - G(\theta)}{G(\theta = 0)}, \quad (9)$$

which reflects the relative change of the conductance with respect to the different orientation of magnetic moments in FM electrodes, an quantity being measurable experimentally. Within the framework of the above formalism, one may investigate the effect of nonmagnetic impurities and the effective masses of conduction electrons on the conductance in F-N-F junctions.

III. EFFECT OF NONMAGNETIC IMPURITIES

To investigate the effect of nonmagnetic impurities on the conductance of F-N-F junctions, we have to make proper assumptions. First, we take $m_1^* = m_2^* = m_3^* = m$, and suppose the two FM electrodes the same, i.e. $|\mathbf{h}_L| = |\mathbf{h}_R| = h$. Then, without loss of generality the coefficients of δ -like impurity potentials at the interfaces are taken as $\gamma_1 = \gamma_2 = \gamma$. We have found that $\gamma_1 \neq \gamma_2$ does not alter qualitatively the behaviors observed. The Fermi energy of the normal metal layer is assumed to be the same as in FM electrodes.

We find that the conductance depends strongly on the relative orientation of magnetizations of FM electrodes, as shown in Fig.2. It is observed that for given d (the thickness of the normal metal layer) and γ (the amplitude of the impurity potential), the conductance is the largest at $\theta = 0$, while at $\theta = \pi$ the conductance reaches the smallest, resurging the spin-valve effect. However, one may note that the conductance is not zero as $\theta = \pi$,

indicating the spin-valve effect is imperfect. This is because in the two-band model the spins in the left FM electrode are not perfectly polarized, there is a portion of electrons with spin down at the Fermi level available, leading to a small current flowing through the junction even if the magnetizations in two FM electrodes are antiparallel, a result quite close to the realistic situation. With increasing θ to π the conductance $G(\theta)$ is monotonically decreasing, while $JMR(\theta)$ is monotonically increasing. In experiments, people are usually interested in the quantity $JMR \equiv JMR(\theta = \pi)$. Without particular specification the JMR refers to $JMR(\pi)$ hereafter.

The effect of impurity on the conductance is shown in Fig.3 for $\theta = \pi/3$ for an example. One may see that at a given Fermi energy (e.g. $E_F = 2.5eV$) with increasing γ the conductance G is first decreasing to a minimum, then increasing to a maximum, and then decreasing to zero. When the energy barrier produced by impurities is high enough, the conductance tends to zero, which is quite reasonable in physics, because in this situation the electrons cannot overcome the impurity-barrier to tunnel through the junction. It is interesting to note that G has a maximum at a certain value of γ , suggesting that the resonant tunneling occurs in this case. This could be viewed as a kind of the impurity-induced resonant tunneling. As the impurity potentials in our model are simulated by the double- δ potential barriers, in the region of normal metal layer there might be some quasi-bound states under certain conditions. The appearance of the quasi-bound states is a consequence arised from both the double- δ potential barriers at two interfaces and the quantum size effect of the middle metal film. When the incident energy of electrons matches approximately the level of the quasi-bound states, the resonant tunneling occurs, manifested by the occurrence of the peak of the conductance versus γ . For other values of E_F , the conductance has the similar behaviors, in spite of positions of maxima being different. From Fig. 3, one may observe that the conductance is oscillating with the Fermi energy.

We also study the JMR versus γ , as shown in Fig.4. It is seen that the JMR is non-monotonous increasing with γ . At low E_F (e.g. $2.4eV$) the JMR shows one peak, and with increasing E_F (e.g. $2.6eV$) the JMR has two peaks. When E_F takes a larger value (e.g. $2.7eV$) only one peak of the JMR is left, which is a consequence of the conductance oscillating with the Fermi energy, leading to that the resonant positions of the JMR depends strongly on the magnitudes of Fermi energies. At larger γ , the JMR saturates to a constant. Furthermore, one may observe that the JMR is negative for some low γ and low E_F . This is not difficult to understand by noting the fact that the spin-up and spin-down electrons in Region 1 have the same incident energies but with different wave vectors, and the transmissivity $T_{p\sigma}(\theta)$ is oscillatory increasing with increasing E_F . At some regimes of low γ and E_F , it is found that $T_{p\uparrow}(0) - T_{p\uparrow}(\pi) > 0$ but $T_{p\downarrow}(0) - T_{p\downarrow}(\pi) < 0$, while the absolute value of the latter is greater than the former, resulting in that the conductance G of parallel alignment of magnetizations is smaller than that of antiparallel alignment at some low E_F and γ , which finally gives rise to the negative JMR . This is actually a result of the two-band model. The JMR is oscillating with the Fermi energy, as shown in Fig.5. When $\gamma = 0$, the JMR is symmetrically oscillating with respect to zero axis. This can be readily understood by taking the two-band feature into account. With increasing γ , the JMR becomes asymmetrically oscillating with more oscillating peaks. Such behaviors are closely related to the quasi-bound states induced by impurity barriers. If E_f is very large, the spin-dependent effect will be smaller, leading to the JMR approaching to zero with

increasing E_f .

The dependence of the JMR on the thickness of the normal metal layer is depicted in Fig. 6. It can be seen that the JMR is oscillating with the thickness d . In absence of the impurity potential, the JMR is symmetrically oscillating with increasing the thickness with one oscillation period. This phenomenon can be of quantum origin, and more specifically, of the quantum-size effect, which has been noted before for the GMR in a one-band model [25] and in double tunnel junction structure [16]. With increasing γ , the oscillation period becomes two, which is closely related to the impurity-induced resonant tunneling or the quasi-bound states. It is interesting to note that the positive and negative JMR effect was also found in the giant magnetoresistance of F-N-F system [25], as well as in N/F/I/F/N structure [26].

IV. EFFECT OF EFFECTIVE MASSES

Now we turn to consider the case that the electrons in the three layers have different effective masses. The solutions of Schrödinger equation have the same forms as Eqs. (2) - (4). However, the boundary conditions are changed. At the interface $x = 0$, it is

$$\psi_1(0) = \psi_2(0); \quad \frac{d\psi_2(0)}{dx} - q_1 \frac{d\psi_1(0)}{dx} = \mu_1 \psi_2(0), \quad (10)$$

and at the interface $x = d$, it becomes

$$\psi_2(d) = \Re\psi_3(d); \quad q_2 \frac{d\psi_2(d)}{dx} = \Re\left[\frac{d\psi_3(d)}{dx} - \mu_2 \psi_3(d)\right]. \quad (11)$$

Recall that $q_1 = \frac{m_2^*}{m_1^*}$, $q_2 = \frac{m_3^*}{m_2^*}$, $\mu_1 = \frac{2m_2^* \gamma_1}{\hbar^2}$, and $\mu_2 = \frac{2m_3^* \gamma_2}{\hbar^2}$. Note that $q_1 \neq q_2$ and $\mu_1 \neq \mu_2$ here. The coefficients contained in the wave functions are given in the Appendix. As the effective masses are different in three regions, the transmissivity, according to its definition $T_{p\uparrow} = j_3/j_1 = \frac{m_1^*}{m_3^*} (\text{Im} \sum_{\sigma} \psi_{\sigma}^* (d\psi_{\sigma}/dx))$, has the form of

$$T_{p\uparrow} = \frac{m_1^* R_{\downarrow}^*(\theta) R_{\downarrow}(\theta)}{m_3^* 4(a_3 - a_4)^2} \left[\frac{k_{3\uparrow}(c_{31}^2 + c_{32}^2)}{\sin^2 \frac{\theta}{2}} + \frac{k_{3\downarrow}(c_{61}^2 + c_{62}^2)}{\cos^2 \frac{\theta}{2}} \right]. \quad (12)$$

$T_{p\downarrow}$ has the same expression as Eq.(12) but with $k_{1\uparrow}$ and $k_{1\downarrow}$, $k_{3\uparrow}$ and $k_{3\downarrow}$ interchanged. The total transmissivity in the two-band case is still $T_p(\theta) = T_{p\uparrow}(\theta) + T_{p\downarrow}(\theta)$. The conductance $G(\theta)$ and the JMR are also defined as Eqs. (8) and (9). To investigate the effect of the effective masses of electrons on the transport properties in F-N-F junctions, in the following we shall assume the same values of parameters (except for $q_1 \neq q_2$ and $\mu_1 \neq \mu_2$) as those in Sec. III. In this case, the wavevectors are different for different effective masses.

The γ - and E_F -dependences of the conductance G for different effective masses are plotted in Figs. 7 (a) and (b), respectively, where we have taken m_2^* as a scale for effective masses. It is seen that compared with Fig. 3 the effect of the effective masses on the conductance versus γ and E_F is quite dramatic. From Fig. 7(a) one may observe that for a given m_1^* the conductance G versus γ is monotonous decreasing for smaller m_3^* but shows resonant peaks for larger m_3^* , namely, when the ratio m_1^*/m_3^* is larger, the conductance versus

γ shows no resonant peaks, implying that the effect of the effective masses smears out the impurity-induced resonant tunneling, while m_1^*/m_3^* is near unity, the sharp peak appears in the curve of G vs. γ , and the impurity-induced tunneling recovers. This observation might be related to the quasi-bound states induced by impurities. The conductance G versus the Fermi energy is oscillating, but the behavior is quite different for different effective masses, as shown in Fig. 7(b). There are two notable characters about G varying with the Fermi energy, namely, the oscillating amplitudes of G for $m_1^*/m_3^* = 1$ are always larger than those for $m_1^*/m_3^* \neq 1$, and the conductance is increasingly oscillating with increasing the Fermi energy.

In order to figure out the effect of the effective masses on the JMR , we plot the JMR versus m_3^* for different m_1^* 's, as shown in Fig. 8, where we have taken $\gamma = 0$ for simplicity. It is seen that the JMR exhibits maxima when the condition $m_1^* \approx m_3^*$ is satisfied, which is clearly illustrated in the inset of Fig. 8, where the contour plot for the maximum JMR in the $m_1^*-m_3^*$ plane is presented. Away from this condition, the JMR is sharply increasing for smaller m_3^* and decreasing for larger m_3^* . This result shows that to get larger JMR one may do the best to choose those ferromagnetic metals with almost the same effective masses of electrons to fabricate the two FM electrodes in a spin-valve. The smaller the difference of the effective masses in the two FM electrodes has, the larger the JMR is.

We have also studied the thickness of the normal metal dependence of the JMR for different m_1^* and m_3^* , as depicted in Fig. 9, where we have taken $\gamma = 0$. In comparison to Fig. 6, one may find that different effective masses would lead to different oscillating behaviors of the JMR . In the upper panel of Fig. 9 where $m_1 = 0.05$, with increasing m_3^* the periodic oscillations of the JMR with $k_F d$ becomes quite different, and when $m_3^* > 1$ the JMR becomes negative. In the middle panel of Fig. 9 where $m_1^* = 1$, one may find that except $m_3^* \approx m_1^*$ the oscillation amplitudes are much suppressed as the ratio m_1^*/m_3^* is much larger or smaller than one. In this case the JMR is negative when m_3^* is smaller. In the lower panel of Fig. 9 where $m_1 = 10$, the situation is just opposite to the case in the upper panel, namely, with increasing m_3^* the oscillating JMR becomes positive from negative. It appears that the sign of the JMR is primarily controlled by m_1^* . As mentioned above, the cause for the oscillation of the JMR with the thickness of the normal metal layer stems from the quantum-size effect, while the oscillation period and amplitude are remarkably affected by the effective masses of electrons, i.e. m_1^* and m_3^* .

To get the knowledge of the resultant effect of both impurity and effective masses on the JMR , we present the results shown in Figs. 10. It is observed that for a given $m_1^* = 0.05$ the JMR is increasing to a maximum due to the impurity-induced tunneling, then decreasing to a minimum, and then increasing to saturate with increasing γ , and those maxima and minima are decreasing with increasing m_3^* , as shown in Fig. 10 (a). With slightly increasing m_1^* , the behaviors of the JMR versus γ and m_3^* are not altered so much, but the resonant positions are changed for different m_1^* 's, as presented in Fig. 10 (b). When m_1^* is larger (e.g. $m_1^* = 5$), the situation changes. Though the behaviors of the JMR versus γ are qualitatively similar for $m_3^* < 1$, two dips appear for $m_3^* > 1$, and those maxima and minima are increasing with increasing m_3^* , as given in Fig. 10 (c). It is indicated that even in the presence of impurities the difference of the effective masses between the left and the right FM electrodes would yield dramatic effect on the behaviors of the JMR . To obtain larger JMR , the proper ratio m_1^*/m_3^* should be carefully chosen.

V. SUMMARY

Based on a two-band model in this paper, we have investigated the effects of nonmagnetic impurities and effective masses of electrons in FM and normal metallic layers on the spin-dependent transport in a F-N-F hybrid structure by treating the system as a quantum-mechanical system. It is observed that both impurities and effective masses have remarkable effects on the conductance and the *JMR* as well. The spin-valve effect, though imperfect due to the two-band feature, is recovered for low impurity barriers, while it becomes less obvious for high barriers. The so-called impurity-induced resonant tunneling is clearly seen in the F-N-F system. The reason for this property is that the quasi-bound states induced by impurities are formed in this system, and if the incident energy meets with the quasi-bound energy, the resonant tunneling occurs, leading to peaks observed in the curve of the conductance versus the amplitude of the impurity potential. It is found that the *JMR* is oscillating with the amplitude of the impurity potential, the incident energies of electrons, as well as the thickness of the normal metallic layer. The impurity is also observed to influence remarkably the oscillating amplitudes and periods of the *JMR*. The effective masses of electrons in the three layers were found to have significant effects on the conductance and the *JMR*. It is demonstrated that the difference between the effective masses would tend to suppress the amplitudes of the conductance, namely, the larger the difference, the smaller the amplitude of the conductance. In other words, a smaller difference of the effective masses in the two FM electrodes would give rise to a larger amplitude of the *JMR*, suggesting that to get larger *JMR* one ought to choose those FM materials with almost identical effective masses of electrons. We have also found that the effective masses affect considerably the oscillating periods, amplitudes, as well as the positions of resonant peaks of the *JMR*. Recently magnetic semiconductors are used to be the injector of electrons in both resonant tunneling diodes [20] and light-emitting diodes [21]. Magnetic semiconductor has both properties of semiconductor and ferromagnet, and in these systems the effective mass of conduction electrons would have considerable effect on the transport properties. Therefore, our above discussion would be meaningful, and the reported results could be examined experimentally. Here we would like to point out that although we do not incorporate factors like spin-flip scatterings from magnons and magnetic impurities, as well as the spin accumulation, our obtained results are expected to shed some useful light on the spin-dependent transport in F-N-F hybrid junctions. How to develop a microscopic theory which includes properly the effects of correlations between electrons, is a challenging issue, which is now in progress.

ACKNOWLEDGMENTS

We thank Dr. Z.C. Wang for useful discussions. This work is supported in part by the National Natural Science Foundation of China (Grant No. 90103023, 10104015), the State Key Project for Fundamental Research in China, and by the Chinese Academy of Sciences.

APPENDIX

In this Appendix, the coefficients introduced in solving the Schrödinger equations in Secs. II and IV are collected here without giving detail derivations.

$$R_{\uparrow} = k_{1\uparrow}^{-1/2} \frac{c_3 c_4 + c_1 c_6 \tan^2 \frac{\theta}{2}}{c_3 c_5 + c_2 c_6 \tan^2 \frac{\theta}{2}}, \quad R_{\downarrow} = k_{1\uparrow}^{-1/2} \tan \frac{\theta}{2} \frac{c_2 c_4 - c_1 c_5}{c_3 c_5 + c_2 c_6 \tan^2 \frac{\theta}{2}};$$

$$A_{\uparrow} = \frac{1}{2} [(a_1^* + 1) k_{1\uparrow}^{-1/2} - (a_1 - 1) R_{\uparrow}], \quad A_{\downarrow} = \frac{1}{2} (1 - a_2) R_{\downarrow},$$

$$B_{\uparrow} = \frac{1}{2} [(1 - a_1^*) k_{1\uparrow}^{-1/2} + (a_1 + 1) R_{\uparrow}], \quad B_{\downarrow} = \frac{1}{2} (1 + a_2) R_{\downarrow};$$

$$C_{\uparrow} = \frac{c_3 R_{\downarrow}}{2(a_3 - a_4) \sin \frac{\theta}{2}}, \quad C_{\downarrow} = \frac{c_6 R_{\downarrow}}{2(a_3 - a_4) \cos \frac{\theta}{2}};$$

where

$$c_1 = c_{11} + i c_{12}, \quad c_2 = c_{21} + i c_{22}, \quad c_3 = c_{31} + i c_{32},$$

$$c_4 = c_{41} + i c_{42}, \quad c_5 = c_{51} + i c_{52}, \quad c_6 = c_{61} + i c_{62},$$

$$c_{11} = 2 \left[\frac{k_{3\downarrow} - q_1 q_2 k_{1\uparrow}}{k q_2} \cos(kd) - \frac{q_1 \mu_2 k_{1\uparrow} - \mu_1 k_{3\downarrow}}{k^2 q_2} \sin(kd) \right],$$

$$c_{12} = 2 \left[\left(\frac{k_{3\downarrow} k_{1\uparrow} q_1 + \mu_1 \mu_2}{k^2 q_2} - 1 \right) \sin(kd) + \frac{\mu_1 q_2 + \mu_2}{k q_2} \cos(kd) \right],$$

$$c_{21} = -2 \left[\frac{k_{3\downarrow} + q_1 q_2 k_{1\uparrow}}{k q_2} \cos(kd) + \frac{\mu_2 k_{1\uparrow} q_1 + \mu_1 k_{3\downarrow}}{k^2 q_2} \sin(kd) \right],$$

$$c_{22} = 2 \left[\left(\frac{k_{3\downarrow} k_{1\uparrow} q_1 - \mu_1 \mu_2}{k^2 q_2} + 1 \right) \sin(kd) - \frac{\mu_1 q_2 + \mu_2}{k q_2} \cos(kd) \right],$$

$$c_{31} = 2 \left[\frac{k_{3\downarrow} + q_1 q_2 k_{1\downarrow}}{k q_2} \cos(kd) + \frac{\mu_2 k_{1\downarrow} q_1 + \mu_1 k_{3\downarrow}}{k^2 q_2} \sin(kd) \right],$$

$$c_{32} = -2 \left[\left(\frac{k_{3\downarrow} k_{1\downarrow} q_1 - \mu_1 \mu_2}{k^2 q_2} + 1 \right) \sin(kd) - \frac{\mu_1 q_2 + \mu_2}{k q_2} \cos(kd) \right],$$

$$c_{41} = 2 \left[\frac{k_{3\uparrow} - q_1 q_2 k_{1\uparrow}}{k q_2} \cos(kd) - \frac{q_1 \mu_2 k_{1\uparrow} - \mu_1 k_{3\uparrow}}{k^2 q_2} \sin(kd) \right],$$

$$c_{42} = 2 \left[\left(\frac{k_{3\uparrow} k_{1\uparrow} q_1 + \mu_1 \mu_2}{k^2 q_2} - 1 \right) \sin(kd) + \frac{\mu_1 q_2 + \mu_2}{k q_2} \cos(kd) \right],$$

$$\begin{aligned}
c_{51} &= -2\left[\frac{k_{3\uparrow} + q_1 q_2 k_{1\uparrow}}{k q_2} \cos(kd) + \frac{\mu_2 k_{1\uparrow} q_1 + \mu_1 k_{3\uparrow}}{k^2 q_2} \sin(kd)\right], \\
c_{52} &= 2\left[\left(\frac{k_{3\uparrow} k_{1\uparrow} q_1 - \mu_1 \mu_2}{k^2 q_2} + 1\right) \sin(kd) - \frac{\mu_1 q_2 + \mu_2}{k q_2} \cos(kd)\right], \\
c_{61} &= 2\left[\frac{k_{3\uparrow} + q_1 q_2 k_{1\downarrow}}{k q_2} \cos(kd) + \frac{\mu_2 k_{1\downarrow} q_1 + \mu_1 k_{3\uparrow}}{k^2 q_2} \sin(kd)\right], \\
c_{62} &= -2\left[\left(\frac{k_{3\uparrow} k_{1\downarrow} q_1 - \mu_1 \mu_2}{k^2 q_2} + 1\right) \sin(kd) - \frac{\mu_1 q_2 + \mu_2}{k q_2} \cos(kd)\right], \\
a_1 &= \frac{q_1 k_{1\uparrow} + i\mu_1}{k}, \quad a_2 = \frac{q_1 k_{1\downarrow} + i\mu_1}{k}, \\
a_3 &= \frac{k_{3\uparrow} + i\mu_2}{k q_2}, \quad a_4 = \frac{k_{3\downarrow} + i\mu_2}{k q_2}.
\end{aligned}$$

REFERENCES

*Corresponding author. E-mail: gsu@gscas.ac.cn.

- [1] R. Meservey and P. M. Tedrow, Phys. Rep. **238**, 173 (1994).
- [2] M.A.M. Gijs and G.E.W. Bauer, Adv. Phys. **46**, 285 (1997).
- [3] G. Prinz, Science **282**, 1660 (1998).
- [4] J.S. Moodera, J. Nassar and G. Mathon, Annu. Rev. Mater. Sci. **29**, 381 (1999).
- [5] M. N. Baibich, J. M. Broto, A. Fert, F. N. V. Dau, F. Petroff, P. Etienne, G. Creuzet, A. Friederich, and J. Chazelas, Phys. Rev. Lett. **61**, 2472 (1988).
- [6] G. E. W. Bauer, Phys. Rev. Lett. **69**, 1676 (1992); V. V. Ustinov and E. A. Kravtsov, J. Phys: Condens. Matter **7**, 3471 (1995); H. E. Camblong, P. M. Levy, and S. Zhang, Phys. Rev. B **51**, 16052 (1995).
- [7] P. M. Tedrow and R. Meservey, Phys. Rev. Lett. **26**, 192 (1971).
- [8] M. Jullière Phys. Lett. A **54**, 225 (1975).
- [9] S. Maekawa and U. Gäfvert, IEEE Trans. Magn. **MAG-18**, 707 (1982).
- [10] J. C. Slonczewski, Phys. Rev. B **39**, 6995 (1989).
- [11] J. Mathon, Phys. Rev. B **56**, 11810 (1997).
- [12] Z.C. Wang, G. Su, Q.R. Zheng and B.H. Zhao, Phys. Lett. A **277**, 47 (2000); Eur. Phys. J. B **19**, 589 (2001); Z.C. Wang, G. Su and S. Gao, Phys. Rev. B **63**, 224419 (2001); Z.C. Wang, G. Su and Q.R. Zheng, Phys. Rev. B **64**, 014407 (2001).
- [13] M. Johnson, and R. H. Silsbee, Phys. Rev. B **35**, 4959 (1987); M. Johnson, Phys. Rev. Lett. **70**, 2142 (1993).
- [14] T. Valet and A. Fert, Phys. Rev. B **48**, 7099 (1993); A. Fert and S. F. Lee, Phys. Rev. B **53**, 6554 (1996).
- [15] D. H. Hernando, Yu. V. Nazarov, A. Brataas and G. E. W. Bauer, Phys. Rev. B **62**, 5700 (2000).
- [16] Zhiming Zheng, Yunong Qi, D. Y. Xing, and Jinming Dong, Phys. Rev. B. **59**, 14505 (1999).
- [17] A. Brataas, Yu. V. Nazarov and G. E. W. Bauer, Phys. Rev. Lett. **84**, 2481 (2000).
- [18] W. Belzig, A. Brataas, Yu. V. Nazarov, and G. E. W. Bauer, Phys. Rev. B **62**, 9726 (2000).
- [19] A. M. Bratkovsky, Phys. Rev. B **56**, 2344 (1997).
- [20] H. Ohno, Science **281**, 951 (1998).
- [21] Y. Ohno, D. K. Young, B. Beschoten, F. Matsukura, H. Ohno, and D. D. Awschalom, Nature (Landon) **402**, 790 (1999).
- [22] M. E. Flatté, and G. Vignale, Appl. Phys. Lett. **78**, 1273 (2001).
- [23] P. M. Levy, K. Ounadjela, S. Zhang, Y. Wang, C. B. Sommers and A. Fert, J. Appl. Phys. **67**, 5914 (1990).
- [24] C. B. Duke, *Tunneling in Solids* (Academic, NewYork, 1969); in *Tunneling Phenomena in Solids*, edited by E. Burstein and S. Lundquist (Plenum, New York, 1969).
- [25] J. Barnas and Y. Bruynseraede, Phys. Rev. B **53**, R2956 (1996).
- [26] X. D. Zhang, B. Z. Li, W. S. Zhang and F. C. Pu, Phys. Rev. B **57**, 1090 (1998).

FIGURE CAPTIONS

Fig.1 The schematic layout of the F-N-F hybrid junction.

Fig.2 The relative orientation (θ) dependence of the conductance for different γ [in atomic unit (au)], where $E_F = 2.7eV$, $|\mathbf{h}_L| = |\mathbf{h}_R| = 1.9eV$, $V_1 = V_2 = 0.06 eV$, $\hbar = 1$, $m = m_1^* = m_2^* = m_3^* = 1$ and $d = 30 \text{ \AA}$.

Fig.3 The γ -dependence of the conductance G for different Fermi energies, where $\theta = \pi/3$. The other parameters are chosen the same as in Fig.2.

Fig.4 The γ -dependence of the JMR for different Fermi energies, where the parameters are chosen the same as in Fig.2.

Fig.5 JMR as a function of E_F for different γ 's. The parameters are chosen the same as in Fig.2.

Fig.6 The thickness dependence of the JMR for different γ 's. The other parameters are chosen the same as in Fig.2.

Fig.7 (a) The γ -dependence of the conductance G for different effective masses; (b) The E_F -dependence of the conductance G for different effective masses, here $\gamma = 0$. Both $\theta = \pi/3$, $m_2^* = 1$, $d = 50 \text{ \AA}$, and the other parameters are chosen the same as in Fig. 2.

Fig.8 The m_3^* -dependence of the JMR for different m_1^* 's, here $m_2^* = 1$ and $\gamma = 0$. Inset: The contour plot for the maximum JMR in m_1^* - m_3^* plane. The other parameters are chosen the same as in Fig. 2.

Fig.9 The thickness dependence of the JMR for different effective masses, where $m_2^* = 1$, $\gamma = 0$, and the other parameters are chosen the same as in Fig.2.

Fig.10 The γ -dependence of the JMR for different m_3^* 's, where $m_2^* = 1$, and the other parameters are chosen the same as in Fig.2. (a) $m_1^* = 0.05$; (b) $m_1^* = 0.5$; (c) $m_1^* = 5$.

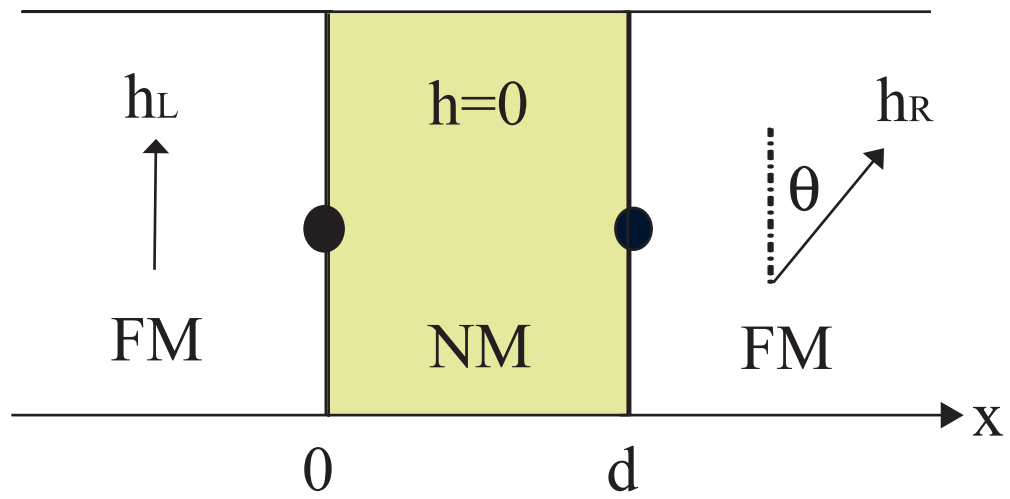


Fig.1 Zhu et al

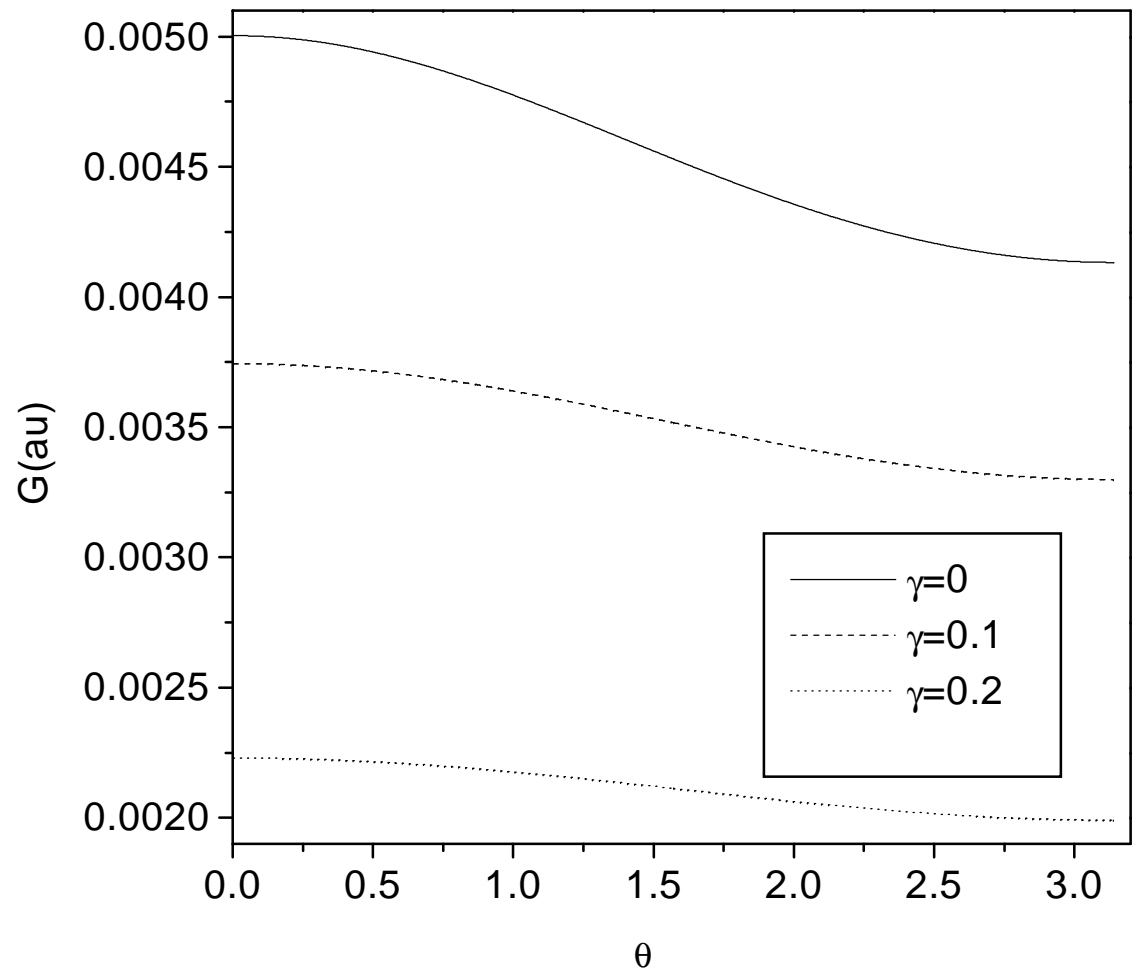


Fig. 2 Zhu et al

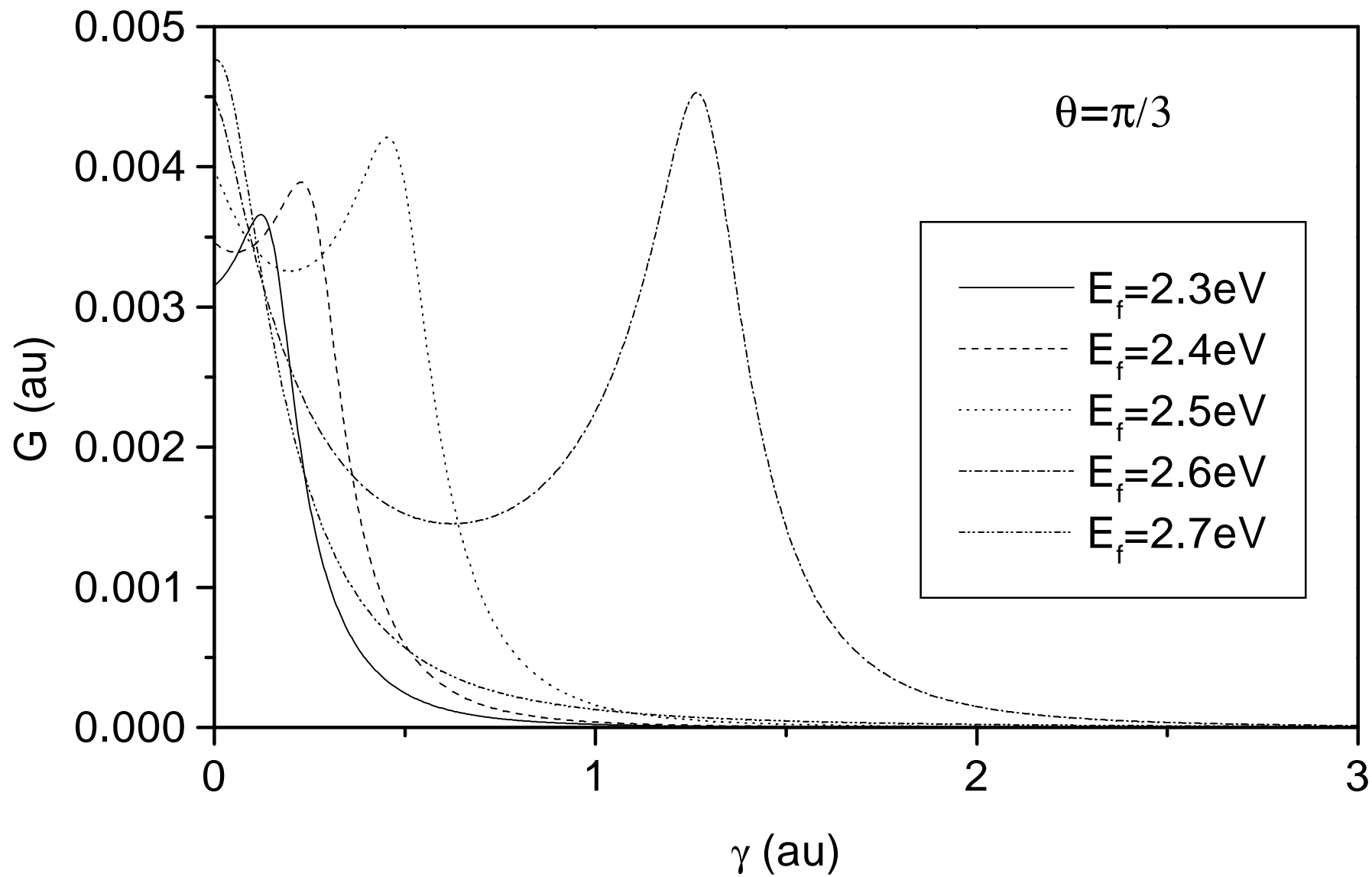


Fig. 3 Zhu et al

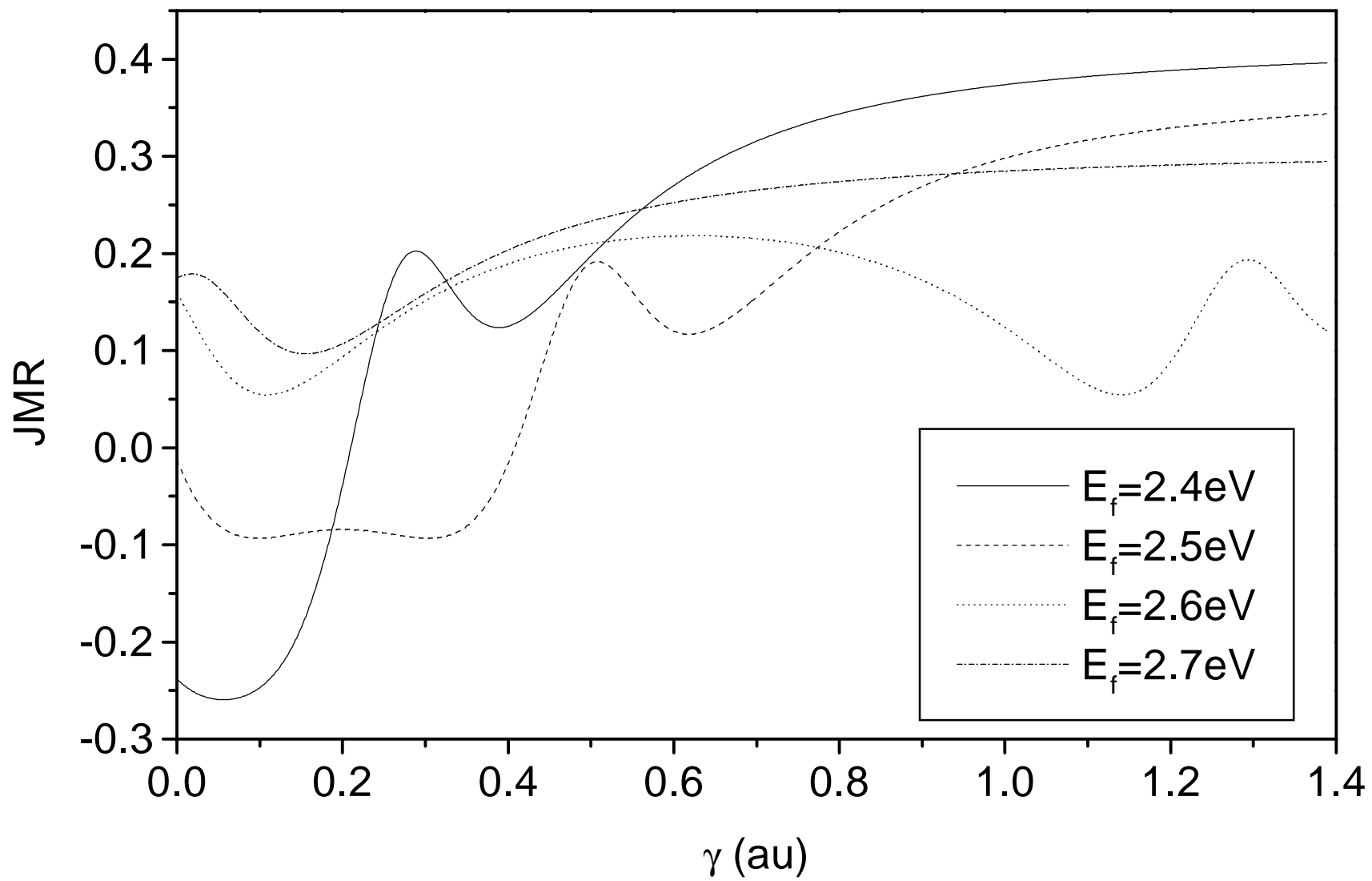


Fig. 4 Zhu et al

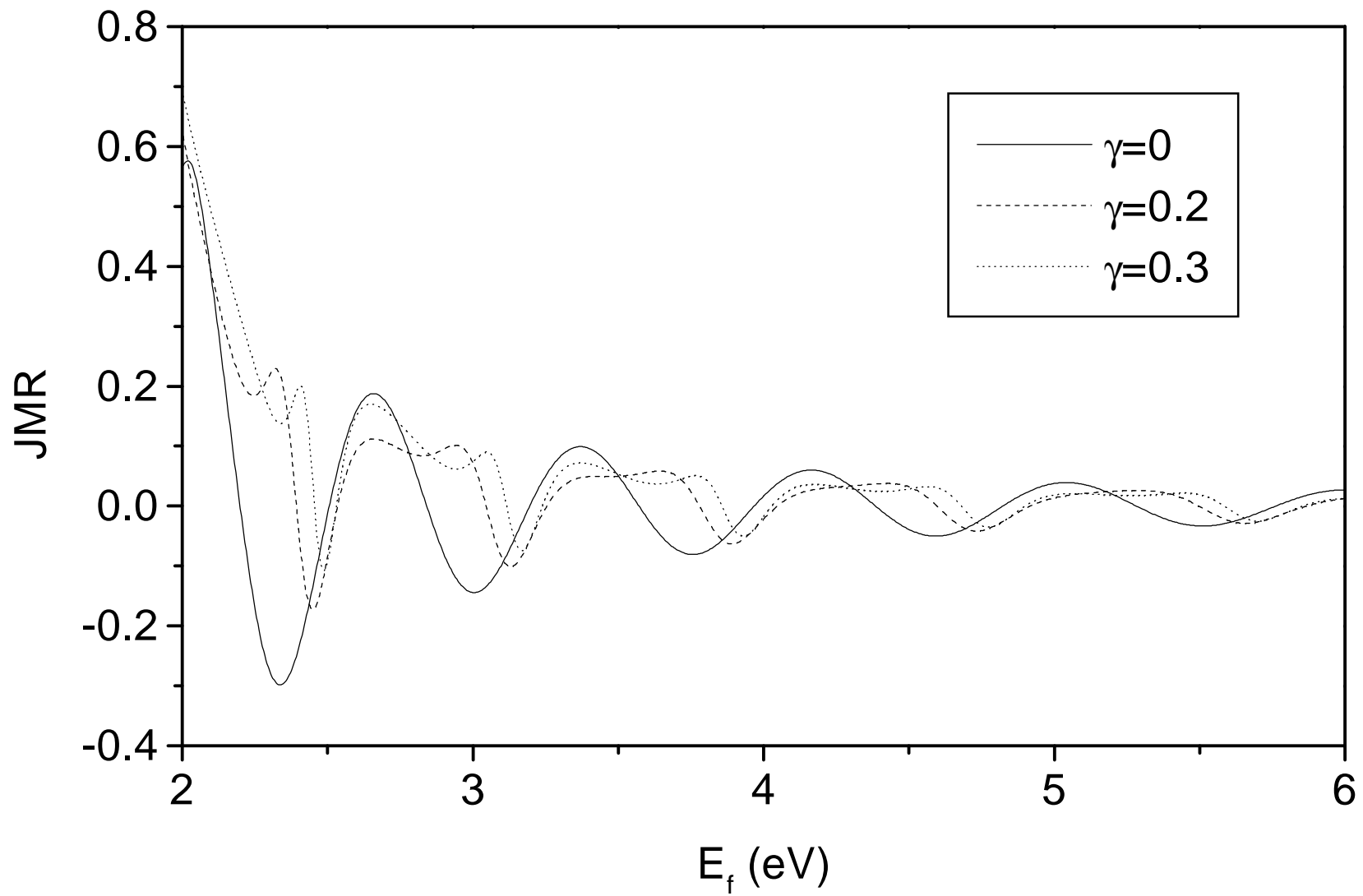


Fig. 5 Zhu et al

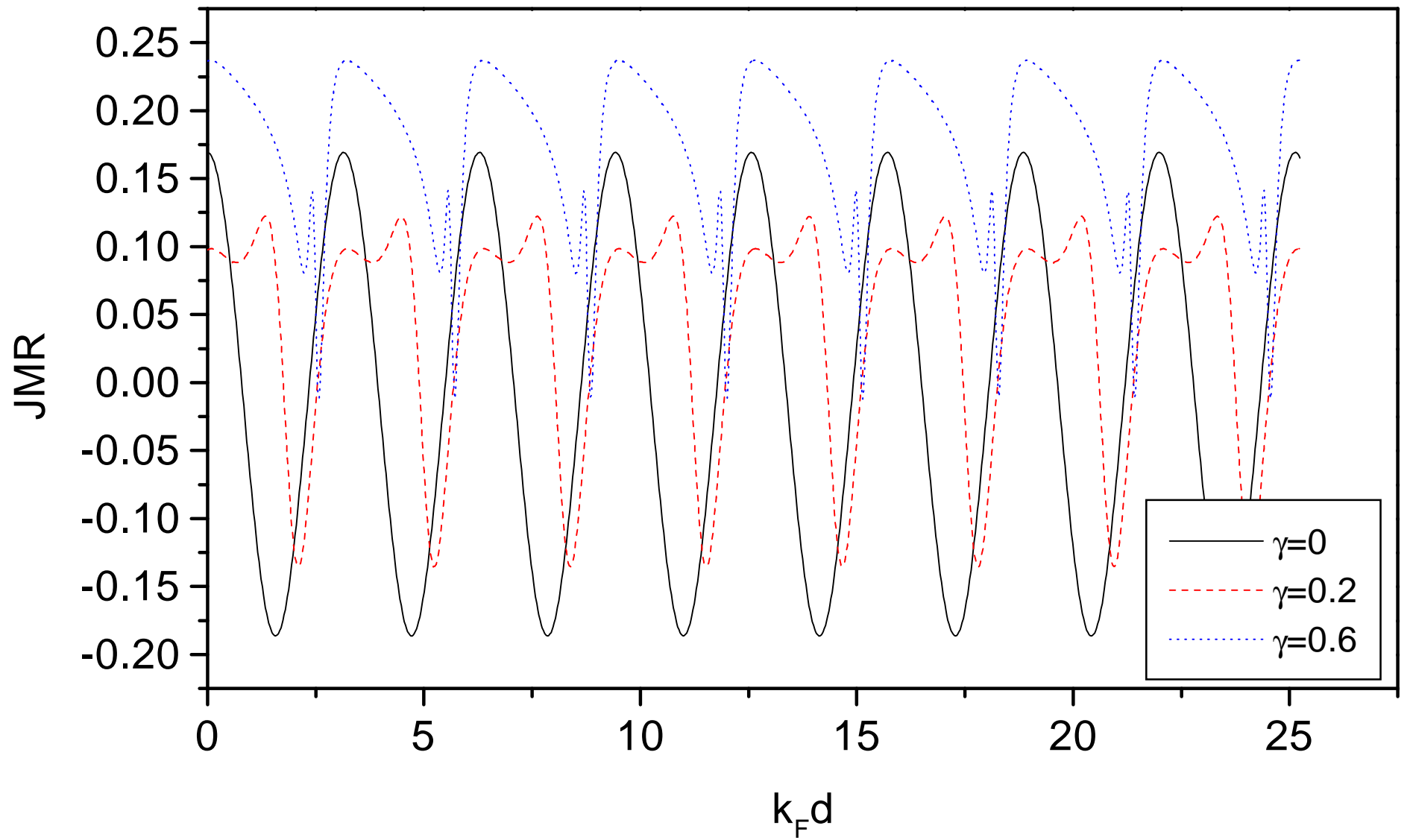


Fig. 6 Zhu et al

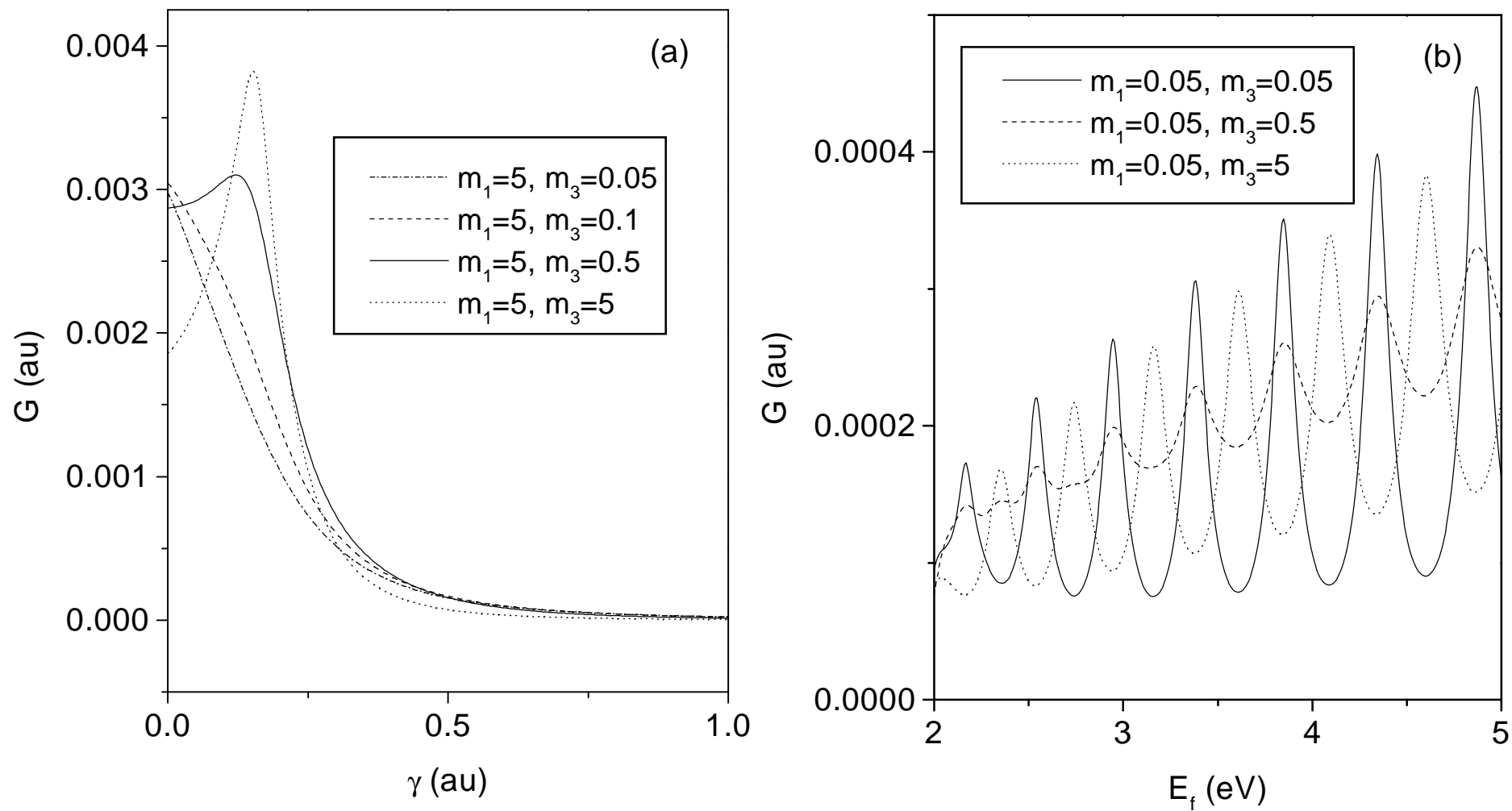


Fig. 7 Zhu et al

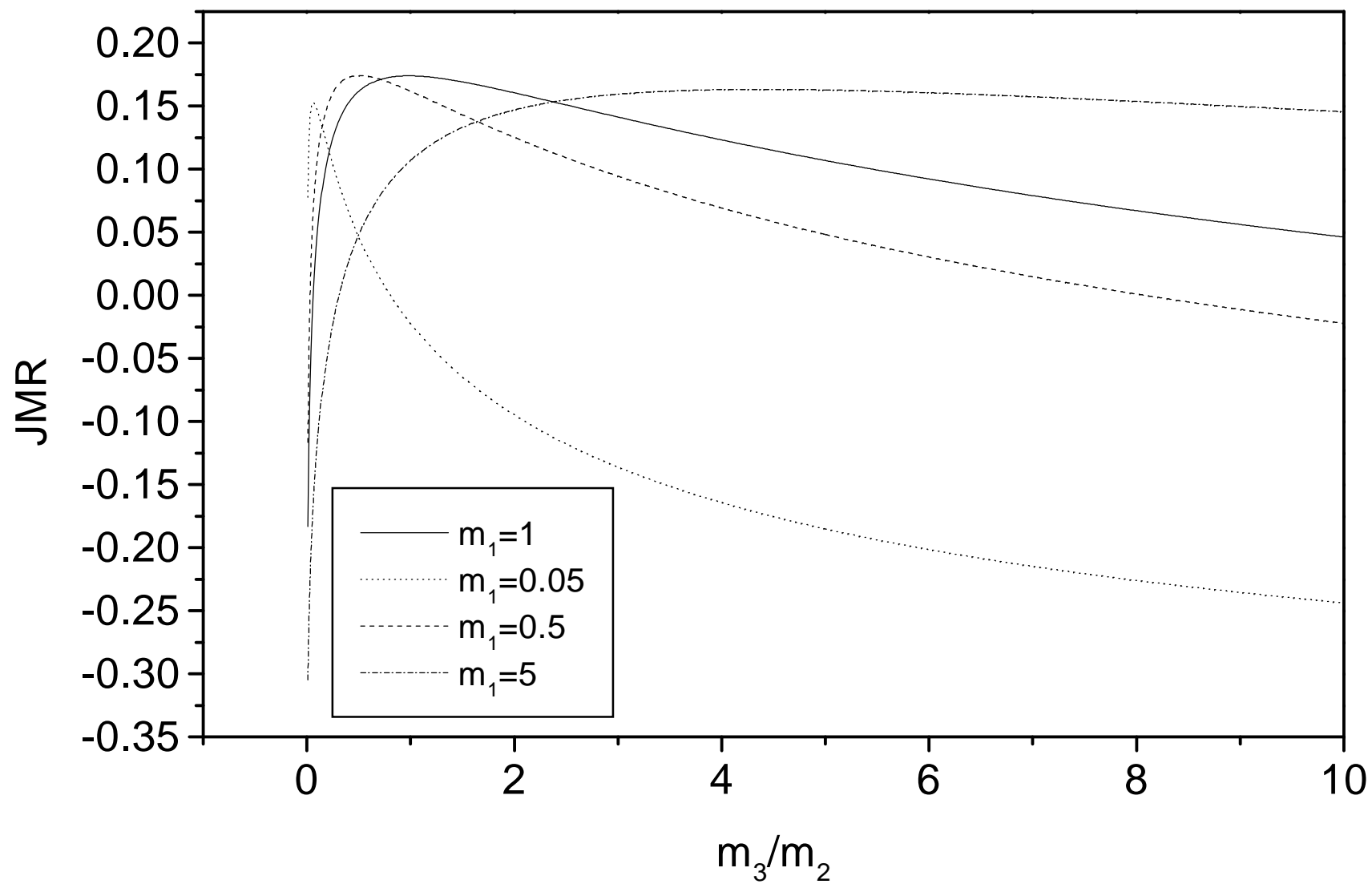


Fig. 8 Zhu et al

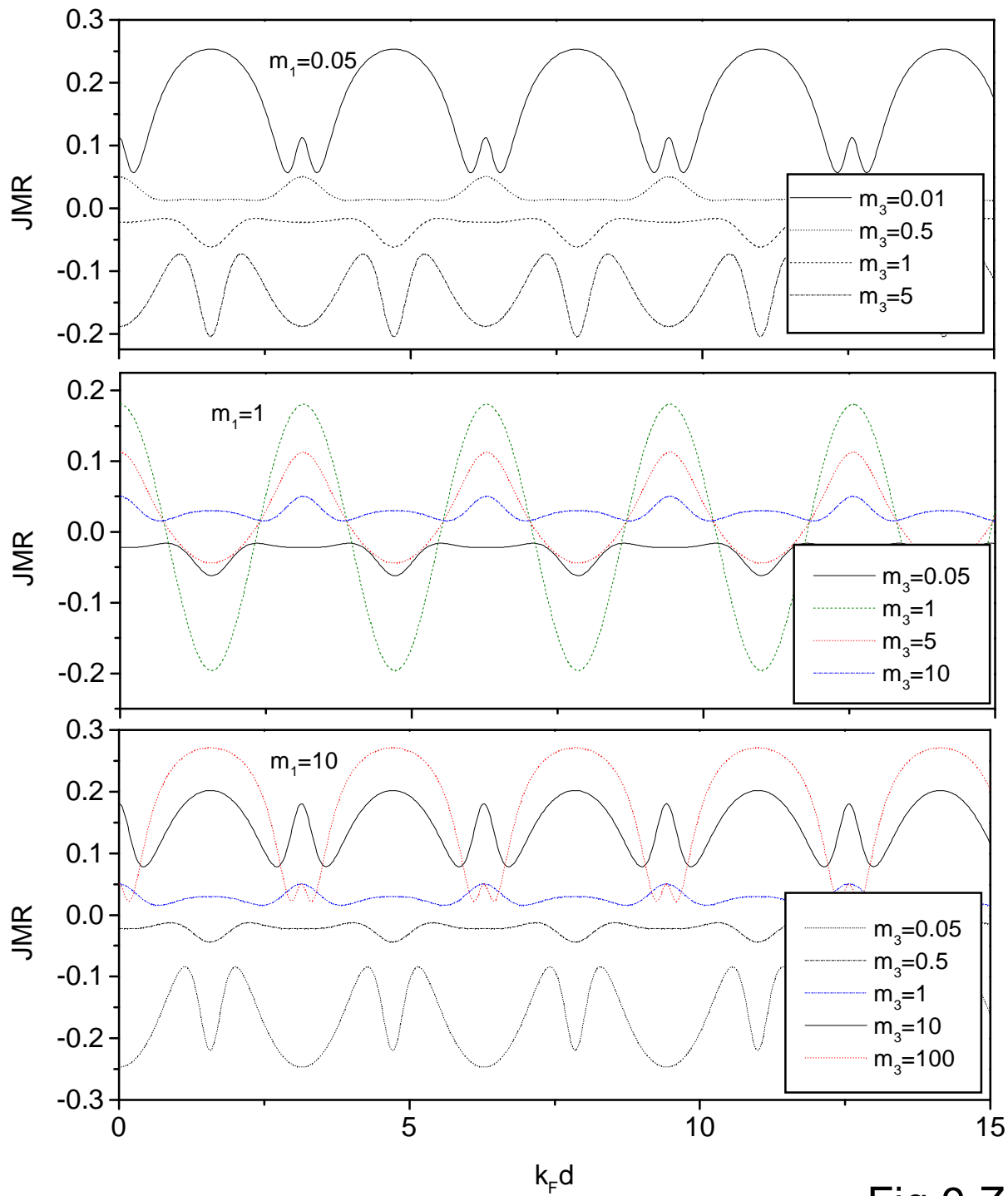


Fig.9 Zhu et al

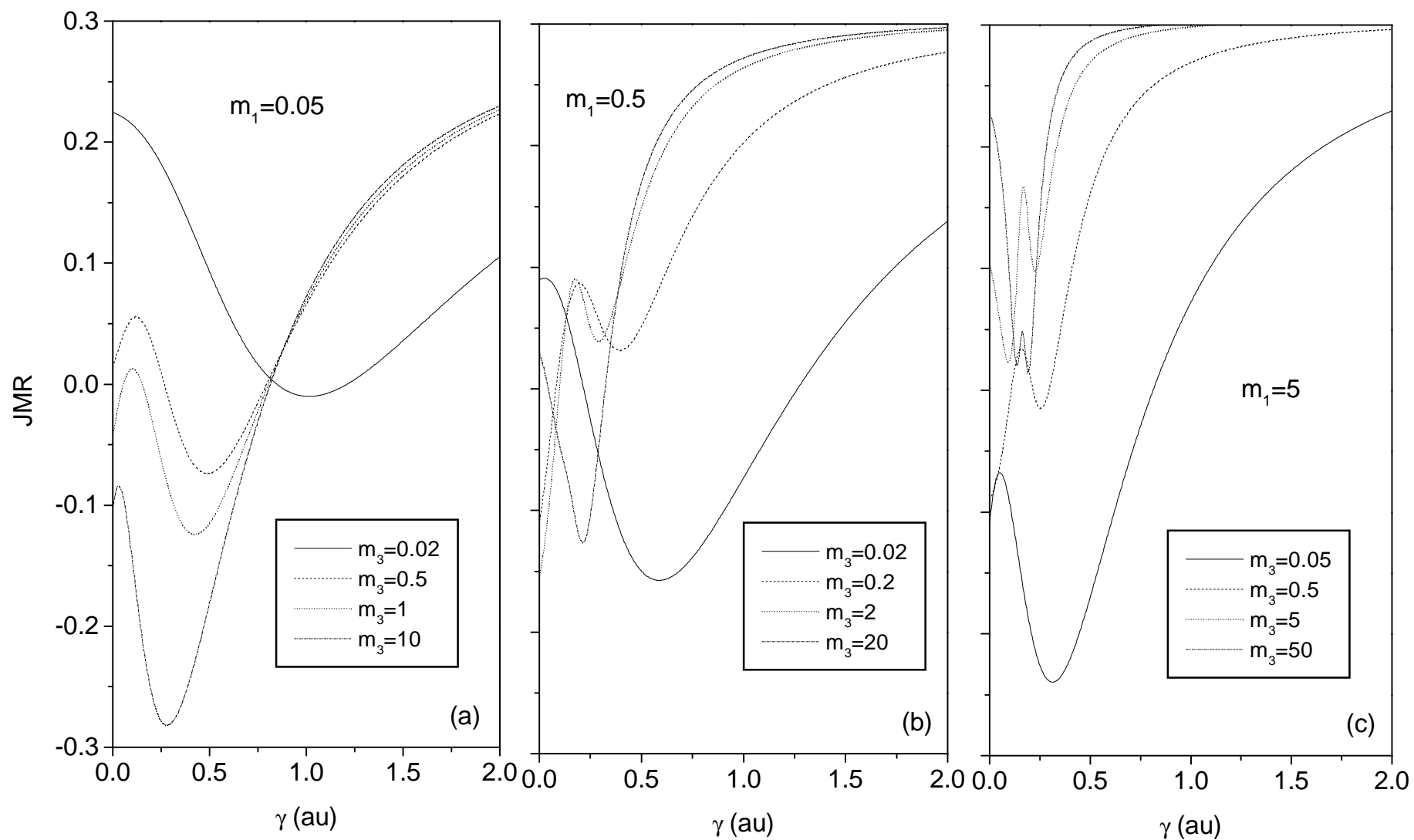


Fig. 10 Zhu et al